Undrained brittleness of sand in triaxial compression and ring shear tests

Abouzar Sadrekarimi
Department of Civil and Environmental Eng.
University of Western Ontario, London, Ontario, Canada
Scott Olson
Department of Civil and Environmental Eng.
University of Illinois, Urbana, Illinois, USA

ABSTRACT
Undrained brittleness index, I_B, is defined as the difference between the peak and critical undrained shear strengths normalized by the peak undrained strength, and indicates soil contractiveness and severity of strain softening. In this study, the results of 25 undrained triaxial compression and 20 constant volume ring shear tests performed on two clean sands and one silty sand are used to evaluate I_B. The results illustrate that I_B increases with initial void ratio and state parameter and is affected by particle shape and particle damage, but is independent of the mode of shear (triaxial compression and ring shear). In addition, I_B appears uniquely related to the ratio of consolidation stress to effective stress at critical state, σ'_c/σ'_{cs}, and critical strength ratio, s_u(critical)/σ'_c, independent of sand type, mode of shear, initial fabric, and particle damage. These relationships suggest an upper bound critical strength ratio of about 0.3.

RÉSUMÉ
L'indice de fragilité non-drainé du sol, I_B, est définie comme la différence entre les forces pics et les forces critiques de cisaillement non-drainé qui est normalisée par la résistance au pic non- drainé . Il indique le contractiveness et la gravité des adoucissement du sol. Dans cette étude, les résultats de25 essais de compression triaxiale non-drainée et 20 essais de cisaillement avec la sonnerie de volume constante sont utilisés pour évaluer l'I_B. Les essais sont faits sur deux des sables propres et un sable limoneux . Les résultats montrent que l'I_B augmente avec l'indice de vide initiale et paramètre d'état et sois influencé par la forme des particules de sable, et le dommage de particules et sois indépendant du mode de cisaillement (compression triaxiale et cisaillement annulaire). Par ailleurs, I_B est uniquement lié au rapport decontrainte de consolidation de la contrainte effective à l'état critique, σ'_c/σ'_{cs}, et le rapport de force critique, s_u(critical)/σ'_c, et est indépendant du type de sable, le mode decisaillement , structure initiale, et le dommage des particules. Ces relations indiquent une limite supérieure ratio lié force critique d'environ 0.3.

1 INTRODUCTION

If a contractive sand is sheared monotonically under globally undrained or constant volume conditions, the effective stress decreases as the specimen attempts to contract under a constant void ratio. During this process, the shearing resistance reaches an undrained peak shear strength [s_u(yield)], which represents the triggering condition for static flow liquefaction (Hanzawa 1980; Vaid and Chern 1983; Vasquez-Herrera et al. 1988; Konrad 1993; Terzaghi et al. 1996; Olson and Stark 2003). After mobilizing s_u(yield), excess porewater pressure increases at a greater rate and strain-softening occurs, continuing until the soil has exhausted its (negative) dilatancy potential and all net particle reorientation and damage are complete. At this "critical state," the soil deforms with a constant volume, constant shear stress, and constant effective stress (Casagrande 1936; Taylor 1948). The locus of void ratio and effective stress pairs at the critical state (e_{cs},σ'_{cs}) is termed the critical state line (CSL). The shearing resistance mobilized at this condition is the undrained critical shear strength, s_u(critical) (Terzaghi et al. 1996).

The normalized difference between the undrained yield and critical strengths is a convenient way to quantify the flow potential of a strain-softening sand. This is commonly defined by the undrained brittleness index, I_B, as (Bishop 1971):

$$I_B = \frac{s_u(yield) - s_u(critical)}{s_u(yield)} \qquad [1]$$

I_B ranges from 0 to 1, where I_B = 1 indicates s_u(critical) = 0 and a highly contractive response and I_B = 0 occurs in dilative sands where no strain-softening occurs.

In this study, I_B and its relevance to liquefaction and critical state concepts is studied using undrained triaxial compression (TxC) and constant volume ring shear (RS) tests.

2 EXPERIMENTAL PROGRAM

Sadrekarimi (2009) performed an extensive series of drained and undrained/constant volume TxC and RS tests

on contractive and dilative specimens of clean Ottawa 20/40 sand (OT), clean Illinois River sand (IR), and silty Mississippi River sand (MR). This study describes the results of OT sand is a commercially-available, medium-grained, uniform, clean, pure quartz sand with rounded particles from Ottawa, Illinois. It has a specific gravity (G_s) of 2.63, and maximum (e_{max}) and minimum (e_{min}) void ratios of 0.679 and 0.391, respectively. IR sand is a medium-grained, uniform, clean, alluvial sediment from the Illinois River, with G_s = 2.63, e_{max} = 0.757, and e_{min} = 0.464. The particles are rounded to subrounded, and consist primarily of quartz with traces of muscovite, chlorite, and hematite. MR sand is a very fine-grained alluvial silty sand with an average fines content of 38% that we sampled near Cape Girardeau, Missouri. It has subangular to subrounded particles, and contains about 70% albite, 21% quartz [both determined by X-ray diffraction], and 5% calcite [determined by dissolution in acid (Raad 1978)]. Its G_s = 2.65, e_{max} = 1.038, and e_{min} = 0.563. Figure 1 presents the average particle size distributions of these sands.

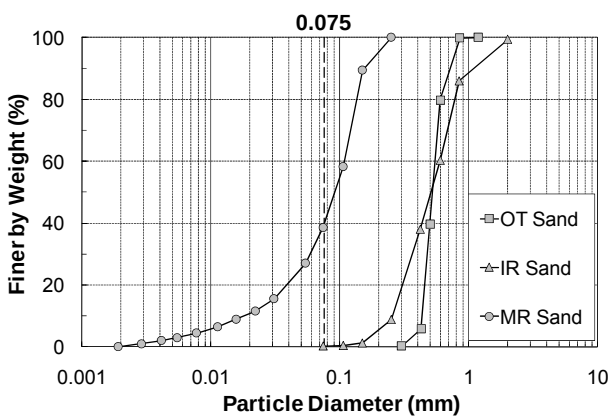

Figure 1. Particle size distributions of the tested sands

Specimens of OT and IR sands were prepared by moist tamping only because air pluviated specimens of these sands dilated during shear. In the moist tamping method, dry sand was moistened and thoroughly mixed with 5% water, and then poured and gently tamped in four layers into the specimen container. The under-compaction method as proposed by Ladd (1974) was used to achieve a relatively uniform density throughout the specimen. In contrast, moist tamped specimens of MR sand deformed excessively during preparation, and therefore MR sand specimens were prepared chiefly by air pluviation and only RS specimen MTMRCV48 was prepared by moist tamping. Moist tamped and air pluviated specimens of MR sand contracted throughout both TxC and RS tests. As discussed by Sadrekarimi and Olson (2008), we anticipate that MR sand was entirely contractive because of its angular fines (making the initial soil fabric more compressible) and its more compressible mineralogy (albite and calcite) compared to the OT (quartz) and IR (quartz and feldspar) sands.

In the air pluviation method, dry sand was poured into a funnel with its tip resting on the bottom of the specimen mould. The funnel was gently raised to deposit the particles with nearly zero drop height. This technique produced the loosest possible structure using air pluviation (Lade et al. 1998) and reduced segregation between the fine and coarse particles. For both preparation methods, we verified specimen uniformity by preparing a number of specimens in several lifts and measuring the weight and height of sand deposited in each lift and at different locations along the circumference of the RS specimens. We observed that the void ratio of an individual lift deviated by less than 5% from the average void ratio of the entire specimen.

Table 1. Specifications of the undrained TxC tests performed in this study

Test No.[1]	*Initial* σ'_c (kPa)	*Initial* e_c	*Yield* s_u (kPa)	*CS_o* s_u (kPa)
MTOTUN83	571	0.724	123	29
MTOTUN52	361	0.787	65	6
MTOTUN103	711	0.700	170	77
MTOTUN102	704	0.770	115	10
MTOTUN42	290	0.796	48	4
MTOTUN92	635	0.771	114	12
MTOTUN82	566	0.766	109	14
MTOTUN63	435	0.722	107	27
MTIRUN29	199	0.844	38	2
MTIRUN17	117	0.835	26	3
MTIRUN52	359	0.690	100	65
MTIRUN83	569	0.670	156	106
MTIRUN112	773	0.677	182	87
MTIRUN12	85	0.818	20	4
MTIRUN55	381	0.674	120	91
MTIRUN43	301	0.756	65	12
MTIRUN54	373	0.732	88	29
MTIRUN26	177	0.810	38	4
APMRUN32	221	0.714	38	19
APMRUN62	425	0.636	75	47
APMRUN92	636	0.594	123	83
APMRUN47	326	0.640	60	36
APMRUN39	272	0.662	49	29
APMRUN58	397	0.658	68	35
APMRUN23	161	0.719	29	15

[1] MT and AP in test numbers indicate moist tamping or air pluviation preparation methods, respectively. OT, IR, and MR indicate OT, IR and MR sands, respectively.

The cylindrical TxC specimens were 50.8 mm in diameter and 101.6 mm tall. To minimize end restraint in the TxC tests, two circular pieces of latex with a thin layer of silicon grease spread between them were used on each triaxial platen. The latex sheets had a center hole and the middle area of the porous stones was left clear of grease to freely drain pore water. We followed the backpressure saturation procedure recommended by Bishop and Henkel (1962) to dissolve any remaining air and saturate the specimen until we observed a pore pressure parameter, B, of at least 0.97. Following

specimen preparation and consolidation to an isotropic stress of σ'_c, we closed the drainage lines and sheared the specimen under undrained conditions to an axial strain of 25%. Measured stresses were corrected to account for the increased specimen area during shearing. Table 1 summarizes the preparation methods, consolidation, yield, and critical states of the TxC tests.

Constant volume RS tests were performed using the newly-developed solid confining ring-type RS apparatus designed and built at the University of Illinois (Sadrekarimi and Olson 2009). The RS apparatus has inner and outer diameters of 20.3 cm and 27.0 cm, respectively, and a height of 2.6 cm. The wide sample section (3.3 cm) minimizes wall friction effects. In a RS test, shear strain increases with radius; therefore, failure occurs progressively. We selected confining ring dimensions to reduce stress and strain non-uniformities to a negligible amount at smaller shear displacements by reducing the ratio of the outside to inside confining ring diameters to 1.33 for this RS apparatus that resulted in an error of less than 2% at s_u(yield) due to strain non-uniformity. We note that these non-uniformities become irrelevant at larger shear displacements (Sadrekarimi and Olson 2009).

Table 2. Specifications of the constant volume RS tests performed in this study

Test No.[1]	Initial σ'_c (kPa)	Initial e_c	Yield s_u (kPa)	CS_o s_u (kPa)	CS_c[3] s_u (kPa)
MTOTCV54(1)[2]	375	0.628	100	47	-
MTOTCV21	144	0.680	32	5	4
MTOTCV88	624	0.638	135	23	14
MTOTCV63	452	0.633	108	22	14
MTOTCV54(2)	376	0.687	74	7	6
MTIRCV46(1)	318	0.722	61	13	9
MTIRCV52	367	0.674	94	50	10
MTIRCV75	636	0.643	180	81	20
MTIRCV53	368	0.657	107	31	11
MTIRCV18	124	0.744	26	7	3
MTIRCV56	396	0.691	91	20	11
APMRCV57	378	0.756	79	19	11
APMRCV22	151	0.728	50	17	12
APMRCV43	298	0.709	83	22	20
APMRCV87	602	0.677	187	103	49
APMRCV103	728	0.667	253	130	66
APMRCV89	624	0.685	156	111	31
APMRCV48	355	0.698	109	50	23
MTMRCV48	334	0.742	75	25	10
APMRCV17	128	0.736	41	8	10

[1] MT and AP in test numbers indicate moist tamping or air pluviation preparation methods, respectively. OT, IR, and MR indicate OT, IR and MR sands, respectively.
[2] This specimen was not sheared to CS_c.
[3] CS_o and CS_c were defined from the same test.

In the RS tests, dry air pluviated or moist tamped sand specimens were placed in the annular chamber of the apparatus, consolidated to a normal stress of σ'_c, and sheared to more than 20 m of shear displacement. All specimens were tested dry, as the device does not currently allow measurement of porewater pressure along the sliding surface. A constant volume condition was imposed by locking the apparatus loading plates after consolidating the specimen, and shearing was induced by rotating the bottom disk, which is deeply serrated to prevent slippage. Sadrekarimi and Olson (2009) provide further details of the TxC and RS experiments, specimen preparation, and testing methods. Table 2 provides the preparation methods, consolidation, yield, and critical states for each of the RS tests performed for this study.

Very loose moist tamped specimens of OT and IR sands contracted throughout the TxC (see Fig. 2) and RS (see Fig. 3) tests. Estimating shear strain in RS tests is problematic because of shear band formation; therefore, we used displacements (shear displacement in RS and axial displacement in TxC) rather than strains to illustrate the results in Figs. 2 and 3. At large shear displacement, significant particle damage and crushing occurred within the shear band of the RS tests, while negligible particle damage occurred in the TxC specimens (Sadrekarimi and Olson 2010a). A constant stress state was reached in both modes of shear; however it was maintained to displacements exceeding 2000 cm in the RS tests. For the purpose of this study, we defined the critical state at the flat post-peak minimum value of effective mean stress in TxC at which the stress ratio had reached a reasonably constant value. The loose moist tamped TxC specimens of OT and IR sands as well as the air pluviated TxC specimen of MR sand achieved critical state prior to the end of shearing. This critical state likely represents a state of complete particle rearrangement without significant particle damage, or in other words, the critical state of the original sand gradation (CS_o). Although in some tests (e.g., MTOTUN52 in Fig. 2) the deviator stress exhibits a very gently decreasing trend, extrapolation of this trend shows only a very minor change with further shear displacement. Thus we anticipate that the reported critical state stresses are accurate and reasonable.

As indicated by the values of e_c in Tables 1 and 2, moist tamped specimens could be prepared at void ratios much looser than e_{max} achieved by air pluviation. This was necessary in order to promote contractive behaviour in OT and IR sand specimens and define specific behavioural parameters. The metastable structure of moist tamped specimens replicates cases where for example moist sand is dumped as a fill and subsequently submerged as the water table rises (Olson et al. 2000; Chu and Leong 2003), or loess soils formed by slow dry aggradation of windborne dust held in a loose state by means of pore water suction (Dijkstra et al. 1994). Moreover, using both moist tamping and air pluviation methods, the results presented in this study cover a very wide range of consolidation relative densities, D_{rc} ($-40\% < D_{rc} < 93\%$) with most data at $D_{rc} > 10\%$.

The RS specimens also likely reached a CS_o after shear band formation but prior to significant particle damage occurring. For reference, particle damage consistently became significant after shear displacements of about 7 cm (after the second phase transformation) in dilative specimens and consistently after about 30 cm in contractive specimens, while shear bands formed consistently after shear displacements of about 0.5 cm for

all specimens (Sadrekarimi and Olson 2010a,b). These shear displacements were determined visually during RS tests performed using a Plexiglas outer ring. As illustrated in Fig. 3, a reduced shear stress plateau was reached at 10 – 15 cm of shear displacements in the RS tests that would correspond to CS_o, after which shear stress decreased because of the ensuing particle damage at greater shear displacements. Thus, it can be reasonably assumed that for the loose specimens presented here, complete particle rearrangement would occur shortly after shear banding at shear displacements smaller than about 30 cm.

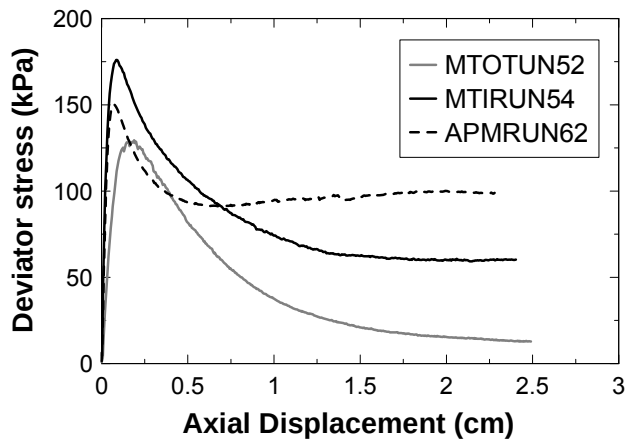

Figure 2. Deviator stress – displacement from TxC tests

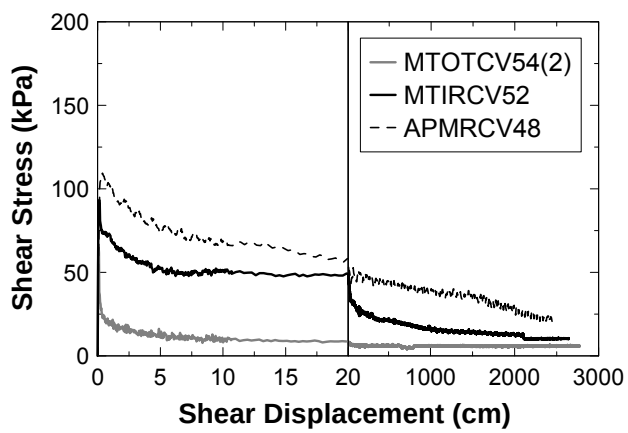

Figure 3. Shear stress – displacement from RS tests

At very large shear displacements (exceeding 10 m) in the RS tests, particle damage and rearrangement/ reorientation were complete and a critical state corresponding to the damaged sand was achieved. The shear resistance typically levelled off at displacements exceeding 10 m and reached an essentially constant value. However, as mass liquefaction often occurs without the formation of a distinct shear band and associated particle damage, Sadrekarimi and Olson (2010a) proposed two definitions of the critical state: (1) the critical state of the original, undamaged sand (CS_o) that is mobilized at relatively small displacements; and (2) the critical state of the damaged (i.e., crushed) sand (CS_c) that is mobilized at very large displacements (often > 10 m). Note that as the complete state of stress is undetermined in RS (similar to the undetermined state of stress in direct shear and direct simple shear tests), and only the state of stress on the failure plane is known, the shear stresses in Fig. 3 correspond to the shear stress, τ_f, measured on the horizontal failure plane.

3 SAND BRITTLENESS

Figure 4 presents I_B values for the undrained strengths reported in Tables 1 and 2 at CS_o (i.e., $I_{B,CSo}$) for the TxC and RS tests, and at CS_c (i.e., $I_{B,CSc}$) for the RS tests.

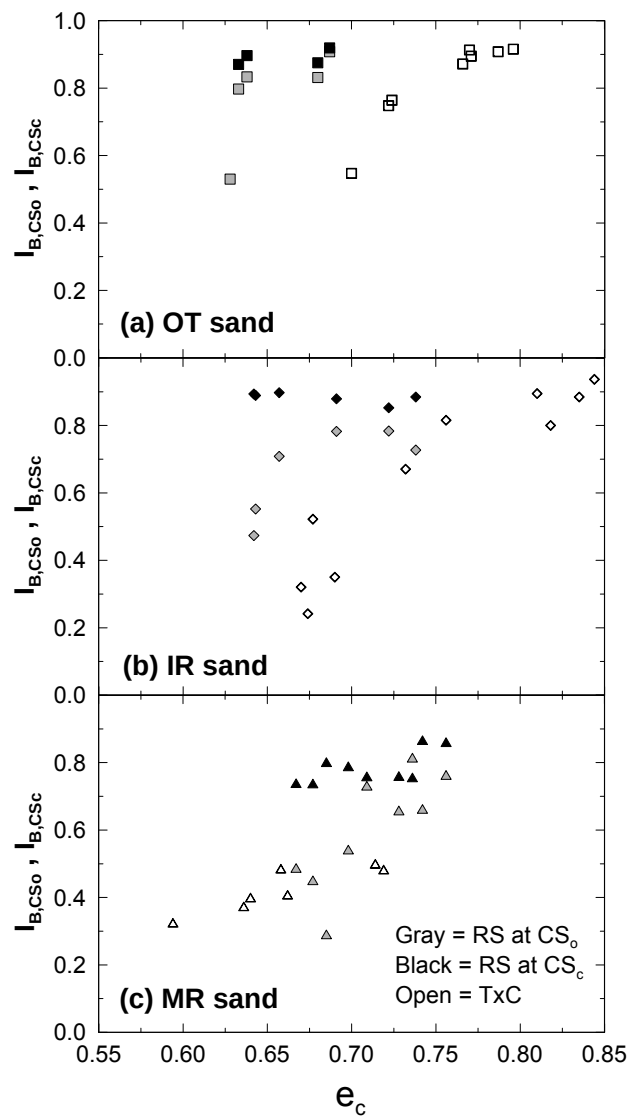

Figure 4. Variations of $I_{B,CSo}$ and $I_{B,CSc}$ with e_c in (a) OT sand, (b) IR sand, and (c) MR sand

These data illustrate that $I_{B,CSo}$ increases with increasing e_c for all of the sands. MR sand shows the least brittle behaviour at CS_o because its higher fines content and angular particles promote a larger s_u(critical) and thus a smaller drop from s_u(yield) to s_u(critical). Several other investigators (e.g., Hird and Hassona 1986; Georgiannou 1988; Pitman et al. 1994) have also observed that I_B decreases with increasing fines content, and at fines contents of approximately 30% to 40%, some sands become ductile (i.e., $I_B \sim 0$). In addition, with the exception of OT sand, $I_{B,CSo}$ values are similar in TxC and RS tests. These results are in contrast with the observations of Wang et al. (2007), who performed partially-drained ring shear tests on silica sand mixed with different amounts of fine silt (loess). They observed that I_B (determined from the minimum shear strength after failure) increased with increasing fines content, and in low fines content (10%) specimens, I_B decreased with increasing e_c. However, for higher fines content (30% and 50%) specimens, I_B values were very similar and roughly constant with e_c. We anticipate that the drainage conditions (i.e., partial drainage) employed by Wang et al. (2007) were responsible for the contrasting results. That is, as e_c increased, excess pore water pressure dissipated more readily, and the post-peak shear strength approached the drained strength. This resulted in I_B decreasing with increasing e_c. On the other hand, increased fines content impeded excess pore water pressure dissipation and led to a lower partially-drained shear strength, and thus a larger I_B value.

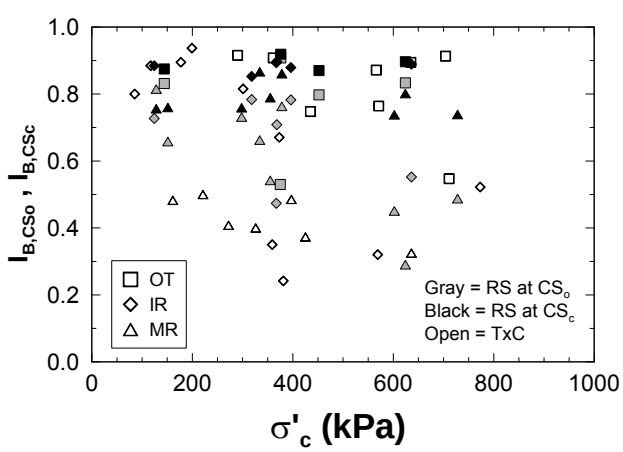

Figure 5. Variations of $I_{B,CSo}$ and $I_{B,CSc}$ with σ'_c in all sands (σ'_c corresponds to effective mean stress and effective normal stress in TxC and RS tests, respectively)

As illustrated in Fig. 4, particle damage and crushing significantly increased the brittleness of each sand (i.e., $I_{B,CSc} > I_{B,CSo}$). After damage occurs, $I_{B,CSc}$ values become nearly independent of e_c, with only MR sand exhibiting a slightly increasing $I_{B,CSc}$ with e_c. The $I_{B,CSc}$ values are presented in terms of void ratio of the undamaged sand after consolidation because it is not possible to determine a priori the severity of damage that will occur in actual geotechnical loading applications. Thus, it is not possible to test a sand that has the proper damaged gradation and properties, and in turn, reporting these $I_{B,CSc}$ data in terms of post-damage parameters is not meaningful.

In contrast to e_c, Fig. 5 illustrates that there is no clear correlation between brittleness indices and σ'_c (note that σ'_c corresponds to effective mean stress and effective normal stress in TxC and RS tests, respectively). This occurs because I_B is primarily affected by e_c (Highter and Tobin 1980; Vaid and Sivathayalan 1996) and slight variations in specimen depositional energies (i.e., tamping force in moist tamped and drop height in air pluviated specimens) produced different initial void ratios and thus different e_c values after consolidation. However, in some geological settings where a sand is deposited in a fairly uniform manner, a unique relationship may exist between e_c and σ'_c, and therefore I_B would depend on σ'_c through its unique relation with e_c. In this case, we expect that at larger σ'_c (i.e. in-situ stress), a sand would become less brittle with greater strain-softening potential.

Figure 6 illustrates the variations of $I_{B,CSo}$ and $I_{B,CSc}$ with D_{rc}. These data show that $I_{B,CSo}$ and $I_{B,CSc}$ (for MR sand) decrease with increasing D_{rc}. For clean OT and IR sands, brittle behaviour is limited to $D_{rc} < 40\%$ whereas the silty MR sand is brittle for $D_{rc} < 93\%$, consistent with data compiled by Olson and Stark (2003). Figure 6 also includes values of $I_{B,CSo}$ for moist-tamped Toyoura sand (Verdugo 1992) sheared in TxC, that are consistent with our data for OT and IR sands. As stated earlier, loose specimens of OT and IR sands ($D_{rc} < 40\%$) were necessary to induce strain-softening response so that s_u(yield) could be measured and I_B calculated. However, these data are used to observe trends and should not be directly used for engineering practice.

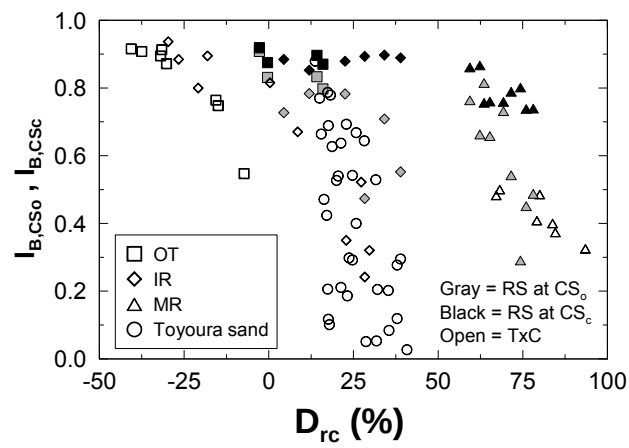

Figure 6. Variations of $I_{B,CSo}$ and $I_{B,CSc}$ with D_{rc} for OT, IR, MR and Toyoura (Verdugo 1992) sands

As anticipated from Fig. 4, $I_{B,CSo}$ for each sand increases with increasing $\psi_{cs,o}$ (Fig. 7a), where $\psi_{cs,o} = e_c - e_{cs,o}$ ($e_{cs,o}$ is the void ratio at CS_o for σ'_c) and is commonly referred to as the state parameter (Roscoe and Poorooshasb 1963; Been and Jefferies 1985). Negative values of $\psi_{cs,o}$ generally correspond to dilative behaviour while positive values correspond to contractive response,

with the severity of strain-softening increasing with increasing $\psi_{cs,o}$. Values of $I_{B,CSc}$ for MR sand also increase with increasing $\psi_{cs,o}$. As suggested by Sladen et al. (1985) and Ishihara (1993), soil state can be also represented by σ'_c/σ'_{cs}. Figure 7b illustrates I_B (both $I_{B,CSo}$ and $I_{B,CSc}$) versus σ'_c/σ'_{cs} for the sands tested here as well as for Banding No. 6 (Castro et al. 1982), Nerlerk and Leighton Buzzard sands (Sladen et al. 1985), and Syncrude tailings sand (Sladen and Handford 1987). As suggested by Sladen et al. (1985), these data illustrate that I_B is a unique function of σ'_c/σ'_{cs} for all sands. In fact, the different I_B - $\psi_{cs,o}$ relationships for each sand in Fig. 7a occurs because of the different CSL slopes of each sand.

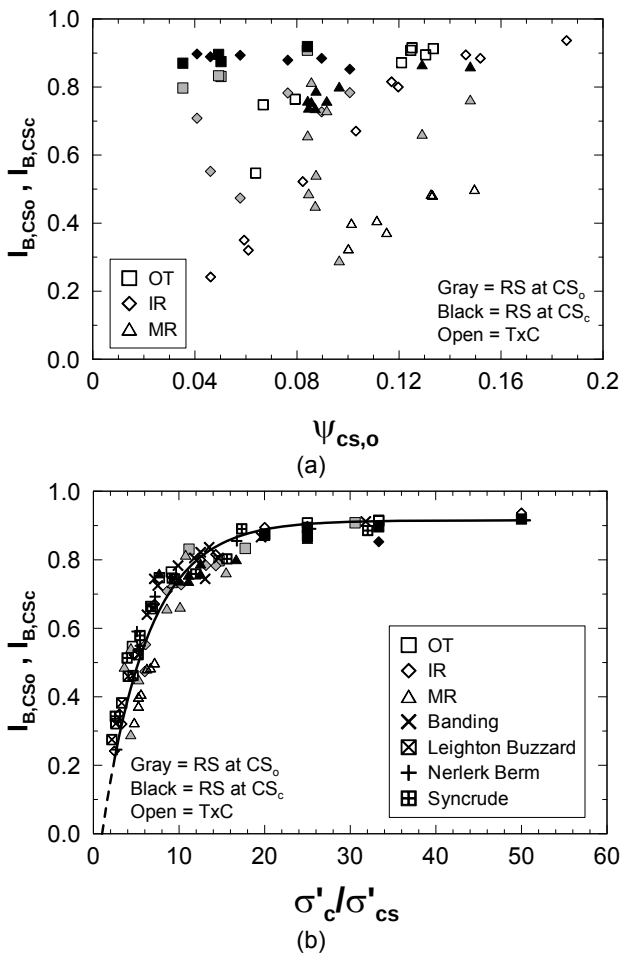

Figure 7. Variations of $I_{B,CSo}$ and $I_{B,CSc}$ with (a) $\psi_{cs,o}$; and (b) σ'_c/σ'_{cs}

The following expression can be used to describe the unique relation between I_B and σ'_c/σ'_{cs} shown in Fig. 7b:

$$I_B = 0.90 - 0.84^{\sigma'_c/\sigma'_{cs}} \qquad [2]$$

Figure 8 presents $s_u(\text{critical})/\sigma'_c$ mobilized in the TxC and RS (at both CS_o and CS_c) with respect to $I_{B,CSo}$ (for TxC and RS at CS_o) and $I_{B,CSc}$ (for RS at CS_c) for OT, IR, and MR sands, as well as for data from TxC tests on Toyoura sand (Verdugo 1992) and several coal mine waste dump sands (Dawson et al. 1998).

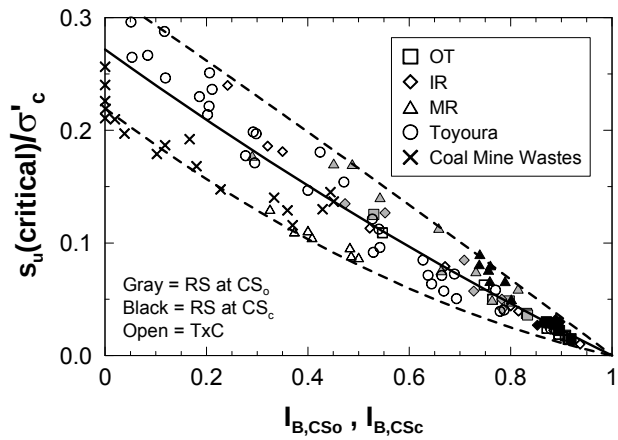

Figure 8. $s_u(\text{critical})/\sigma'_c$ versus $I_{B,CSo}$ and $I_{B,CSc}$ for OT, IR, MR, and Toyoura sands (Verdugo 1992) as well as Greenhills, Quintette, and Fording coal mine waste dump sandy gravels (Dawson et al. 1998)

As illustrated in Fig. 8, a relatively unique relationship appears to exist between $s_u(\text{critical})/\sigma'_c$ and I_B independent of sand type, mode of shear, method of deposition, and particle crushing. As illustrated in Fig. 8, $s_u(\text{critical})/\sigma'_c$ is limited to a value of about 0.3 at $I_B = 0$. The following expression describes the average relation in Fig. 8:

$$\frac{s_u(critical)}{\sigma'_c} = 0.05I_B^2 - 0.32I_B + 0.27 \pm \left(-0.07I_B^2 + 0.02I_B + 0.05\right) \qquad [3]$$

The empirical relationship between e_c, σ'_c, and I_B reported by Highter and Tobin (1980) for the liquefaction susceptibility and post-failure behaviour of garnet, iron, and zinc mine tailings further supports Eq. 3 for most sands and indicates that I_B can be adopted as an index parameter in liquefaction flow failure analysis. Furthermore, although I_B is an index of strength loss after liquefaction, it can be used via Eq. 3 and $s_u(\text{critical})$ to estimate $s_u(\text{yield})$. This may be a valuable tool to assess $s_u(\text{yield})$ in cases where $s_u(\text{critical})$ is back-calculated from the post-failure geometry of a liquefied structure. The average $s_u(\text{yield})$ can be estimated as:

$$s_u(yield) = \frac{\sigma_c'^2}{4.3\sigma'_c - 2.5s_u(critical)} \qquad [4]$$

4 CONCLUSIONS

The undrained brittleness of sand, I_B, defined as the difference between the undrained peak and critical shear strengths normalized by undrained peak shear strength is discussed in this paper. As expected, the largest values of I_B mobilized at CS_o ($I_{B,CSo}$) are associated with the loosest void ratios, independent of mode of shear (TxC and RS). However, particle damage increases brittleness ($I_{B,CSc}$) and $I_{B,CSc}$ reaches nearly constant values for OT and IR sands, while MR sand exhibits a slight increase in $I_{B,CSc}$ with increasing void ratio. We further observed that $I_{B,CSo}$ and $I_{B,CSc}$ (for MR sand) increased as sand state became more contractive as represented by the increasing values of $\psi_{cs,o}$ and σ'_c/σ'_{cs} and a unique correlation was found between I_B ($I_{B,CSo}$ and $I_{B,CSc}$) and σ'_c/σ'_{cs} for all sands. I_B can be potentially used as an index parameter for liquefaction flow failure triggering analysis through its correlation with s_u(critical)/σ'_c, as presented in this paper.

REFERENCES

Been, K. and Jefferies, M. G. 1985. A state parameter for sands. *Géotechnique*, 35(2): 99-112.

Bishop, A. W. 1971. Shear strength parameters for undisturbed and remoulded soil specimens. In Proceedings of the *Roscoe Memorial Symposium*, Cambridge University, Cambridge, Mass., pp. 3 – 58.

Bishop, A. W. and Henkel, D. J. 1962. *The measurement of soil properties in the triaxial test.* St. Martin's Press, Inc., New York, 224 pp.

Casagrande, A. 1936. Characteristic of cohesionless soils affecting the stability of slopes and earth fills. *Journal of Boston Society of Civil Engineers*, 23(1): 13-32.

Castro, G., Enos, J. L., France, J. W., and Poulos, S. J. 1982. Liquefaction induced by cyclic loading. *Report to National Science Foundation*, *No. NSF/CEE-82018,* Washington, D.C.

Chu, J. and Leong, W.K., 2003. Recent progress in experimental studies on instability of granular soil. Proceedings of the *International Workshop on Bifurcation and Instability of Geomaterials*, 2-5 June, Minneapolis, Eds. J.F. Labuz and A. Drescher, Swets & Zeitlinger, B.V., pp. 175-192

Dawson, R. F., Morgenstern, N. R., and Stokes, A. W. 1998. Liquefaction flowslides in Rocky Mountain coal mine waste dumps. *Canadian Geotechnical Journal*, 35(2): 328-343.

Dijkstra, T. A., Rogers, C. D. F., Smalley, I. J., Derbyshire, E., Li, Y. J., and Meng, X. M. 1994. The loess of north-central China: geotechnical properties and their relation to slope stability. *Engineering Geology*, 36: 153 – 171.

Georgiannou, V. N. 1988. Behaviour of clayey sands under monotonic and cyclic loading. Ph.D. Thesis, Imperial College of Science and Technology and Medicine, London, England.

Hanzawa, H. 1980. Undrained strength and stability analysis for a quick sand. *Soils and Foundations*, 20(2): 17-29.

Hird, C. C. and Hassona, F. A. K. 1986. Discussion on: A state parameter for sand. *Géotechnique*, 36: 124 – 127.

Highter, W. H. and Tobin, R. F. 1980. Flow slides and the undrained brittleness index of some mine tailings. *Engineering Geology*, Elsevier, Amsterdam, 16: 71 – 82.

Ishihara, K. 1993. Liquefaction and flow failure during earthquakes. *Géotechnique*, 43(3): 351–415.

Klotz, E.U., and Coop, M.R. 2002. On the identification of critical state lines for sands. *Geotechnical Testing Journal*, ASTM, 25(3): 1 - 14.

Konrad, J. -M. 1993. Undrained response of loosely compacted sands during monotonic and cyclic compression tests. *Géotechnique*, 43(1): 69–89.

Kramer, S.L., Bennetts, B.A., and Wang, C.H. 2002. Sand behavior at large strain in ring simple shear. *In US-Japan seminar on Seismic Disaster Mitigation in Urban Area by Geotechnical Engineering*, Anchorage, Alaska, pp. 291 – 303.

Ladd, R. S. 1974. Specimen preparation and liquefaction of sands. *Journal of Soil Mechanics and Foundation Division*, ASCE, 100(10): 1180-1184.

Lade, P. A., Liggio, C. D., and Yamamuro, J. A. 1998. Effect of non-plastic fines on minimum and maximum void ratios of sand. *Geotechnical Testing Journal*, ASTM, 21(4): 336-347.

Oda, M., Koishikawa, I., and Higuchi, T. 1978. Experimental study of anisotropic shear strength of sand by plane strain test. *Soils and Foundations*, 18(1): 25 – 38.

Okada, Y., Sassa, K., and Fukuoka, H. 2000. Liquefaction and steady state of weathered granitic sands obtained by undrained ring shear tests: a fundamental study of the mechanics of liquidized landslides. *Journal of Natural Disaster*, 22(2): 75 - 85.

Olson, S.M., Stark, T.D., Walton, W.H., and Castro, G. 2000. 1907 static liquefaction flow failure of teh north dike of Wachusett dam. *Journal of Geotechnical and Geoenvironmental Engineering*, ASCE, 126(12): 1184-1193.

Olson, S. M. and Stark, T. D. 2003. Use of laboratory data to confirm yield and liquefied strength ratio concepts. *Canadian Geotechnical Journal*, 40(6): 1164 – 1184.

Pitman, T. D., Robertson, P. K., and Sego, D. C. 1994. Influence of fines on the collapse of loose sand. *Canadian Geotechnical Journal*, 31: 728 – 739.

Raad, A. A. 1978. Carbonates. In: *Manual on Soil Sampling and Methods of Analysis*, J. A. McKeague (ed.), 2nd Ed. Canadian Society of Soil Science, AAFC, Ottawa: 86 – 98.

Riemer, M.F., and Seed, R.B. 1997. Factors affecting apparent position of the steady-state line. *Journal of Geotechnical and Geoenvirionmental Engineering*, ASCE, 123(3): 281 - 288.

Roscoe, K. H. and Poorooshasb, H. B. 1963. A theoretical and experimental study of strains in triaxial tests on normally consolidated clays. *Géotechnique*, 13(1): 12-38.

Sadrekarimi, A. and Olson, S. M. 2008. The importance of mineralogy and grain compressibility in understanding field behavior during liquefaction. *6th International*

Conference on Case Histories in Geotechnical Engineering and Symposium in Honor of Professor James K. Mitchell, Arlington, VA.

Sadrekarimi, A. and Olson, S. M. 2009. A new ring shear device to measure the large displacement shearing behavior of sands. *Geotechnical Testing Journal*, ASTM, 32(3): 197 - 208.

Sadrekarimi A. and Olson, S. M. 2010a. Particle damage and crushing observed in ring shear tests on sands. *Canadian Geotechnical Journal*, 47(5): 497 - 515.

Sadrekarimi, A. and Olson S. M. 2010b. Shear band formation observed in ring shear tests on sandy soils. *Journal of Geotechnical and Geoenvironmental Engineering*, ASCE, 136(2): 366 – 375.

Sladen, J. A., and Handford, G. 1987. A potential systematic error in laboratory testing of very loose sands. *Canadian Geotechnical Journal*, 24(3): 462 – 466.

Sladen, J. A., D'Hollander, R. D., and Krahn, J. 1985. The liquefaction of sands, a collapse surface approach. *Canadian Geotechnical Journal*, 22(4): 564 – 578.

Taylor, D. W. 1948. *Fundamentals of Soil Mechanics*, John Wiley and Sons, New York, 700 pp.

Terzaghi, K., Peck, R. B. and Mesri, G. 1996. *Soil Mechanics in Engineering Practice*. John Wiley and Sons, New York, 549 pp.

Vasquez-Herrera, A., Dobry, R. and Ng. T.-T. 1988. Pore pressure buildup and liquefaction failure of anistropically consolidated sand due to cyclic straining. Proceedings, *Conference on Hydraulic Fill Structures*, Fort Collins, Co. American Society of Civil Engineers: 346-366.

Vaid, Y. P. and Chern, J. C. 1983. Effect of static shear on resistance to liquefaction. *Soils and Foundations*, 23(1): 47-60.

Vaid, Y. P. and Sivathayalan, S. 1996. Static and cyclic liquefaction potential of Fraser River Delta sand in simple shear and triaxial tests. *Canadian Geotechnical Journal*, 33(2): 281-289.

Vaid, Y.P., and Sivathayalan, S. 2000. Fundamental factors affecting liquefaction susceptibility of sands. *Canadian Geotechincal Journal*, 37(3): 592 - 606.

Verdugo, R. 1992. *Characterization of sandy soil behavior under large deformation.* Ph.D. Thesis, University of Tokyo, Tokyo.

Wang, F., Sassa, K., Fukuoka, H., and Tada, T. 2007. Experimental study on the shearing behavior of saturated silty soils based on ring-shear tests., *Journal of Geotechnical and Geoenvironmental Engineering* 133(3): 319 – 333.